Journal of Applied Fluid Mechanics, Vol. 12, No. 6, pp. 1801-1812, 2019.
Available online at www.jafmonline.net, ISSN 1735-3572, EISSN 1735-3645.
DOI: 10.29252/jafm.12.06.29538

Comparison of Interface Description Methods Available in Commercial CFD Software

A. A. Barral Jr.[1], R. B. Minussi[2] and M. V. Canhoto Alves[1†]

[1] *Department of Petroleum Engineering – Santa Catarina State University, Balneário Camboriú, Santa Catarina, 88.336-275, Brazil*
[2] *Centre of Marine Studies – Federal University of Paraná, Pontal do Paraná, Paraná, 83.255-976, Brazil*

†*Corresponding Author e-mail: marcus.alves@udesc.br*

(Received August 16, 2018; accepted January 22, 2019)

ABSTRACT

This study addresses the characteristics of the interpolation functions and interface reconstruction routines for the VOF – Volume of Fluid method available in the commercial CFD software ANSYS-FLUENT. This software was used because it has both implicit and explicit VOF approaches along with diverse interpolation functions. Some of these functions were compared from different viewpoints: the quality of the reconstructed interface; the ability to preserve the initial mass inside the system (numerical diffusion); and the computing time. To undertake the qualitative and quantitative comparisons, a test problem that combines the classical dam break and slosh tank benchmark problems was used. No analytical solution available was found for this problem, in which the most interesting feature is a high interaction between the velocity field and volume fraction, thus making it ideal for addressing the issue of interface smearing. ANSYS-FLUENT permits using 5 interpolation functions for transient simulations: PLIC, CICSAM, HRIC (explicit and implicit) and the UPWIND scheme, and four when performing steady state ones: BGM, modified HRIC, COMPRESSIVE and UPWIND schemes. Both transient and steady state solutions were analyzed in this study, using all the above schemes, except the UPWIND one for steady state simulations. It was found that, for thinner grids, PLIC, CISAM and the explicit HRIC schemes had similar performances concerning the quality of the reconstructed interface and mass conservation. On the other hand, PLIC shows the best results for coarser grids, being the only to conserve mass for all tests. The computation time was similar for all transient simulation (within each grid). Concerning the steady state simulations, which are, in fact, distorted transient simulations, the BGM and the COMPRESSIVE schemes produced similar results, but BGM consumed more computational time.

Keywords: Volume of Fluid; Numerical Diffusion; Interfacial Smearing.

NOMENCLATURE

$\overline{\overline{D}}$	rate of shear tensor
$\dot{m}$	mass transfer flux between phases
p	p[th] phase (when in a subscript) Thermodynamic pressure
q	q[th] phase
S	mass source term
t	time
u	velocity component
$\vec{v}$	velocity
μ	dynamic viscosity
V	velocity modulus
x	coordinate system component
α	volume fraction
δ_S	Dirac's delta function at the interface
κ	interface mean curvature
μ	dynamic viscosity
ρ	specific mass
σ	surface tension
$\mathrm{Re} = \frac{\rho_1 V L}{\mu_1}$	Reynolds number
$Eo = \frac{\rho_1 V L}{\sigma}$	Eötvös number
$Ca = \frac{\mathrm{Re}}{Eo}$	Capillary Number

1. INTRODUCTION

The VOF method can model the flow of two or more fluids by solving a single set of momentum equations and tracking the volume fraction of each of the fluid phase throughout the domain. Typical applications of the VOF model are for immiscible fluid flow and include the prediction of jet breakup, the motion of large bubbles in a liquid, the motion of liquid after a dam break, and the steady or transient tracking of any interphase interface.

For each additional phase to model, a variable must be introduced: the volume fraction of the phase in each computational cell. In each control volume, the sum of volume fractions of all phases must be equal to one. The fields for all variables and properties are shared by the phases and represent volume-averaged values (if the volume fraction of each of the phases is known at each location and time). Thus, the variables and properties in any given cell are either purely representative of one of the phases, or representative of a mixture of the phases, depending upon the volume fraction values. Based on the local volume fraction, the appropriate properties and variables are assigned to each control volume within the domain.

The VOF model has been used in the literature to simulate several complex problems in engineering, such as: the transient behavior of lubricant inside hermetic compressors (Lückmann *et al*., 2009; and Alves *et al*. 2011 & 2013); two phase flows in tubes and ducts (Soleymani *et al.*, 2008; Da Riva and Del Col, 2009; Kashid *et al.*, 2010; Hernandez-Perez *et al.*, 2011; Horgue *et al.*, 2012; Magnini *et al.*, 2013; Ratkovich *et al.*, 2013; Karami *et al.*, 2014; Saad *et al.*, 2014; Bortolin *et al.*, 2014); modeling of the Rayleigh-Taylor Instabilities (Bilger *et al.* 2017); simulation of the dam break problem (Minussi and Maciel, 2012; Caron *et al*., 2015). Although very useful, the VOF model has limitations specially regarding the momentum transfer through the interface (Rezende *et al.*, 2014). Rezende *et al.* (2014) developed a novel approach to close the interfacial modeling for two-phase flow modeling with the VOF method.

The open literature also has several studies dealing with the comparison of several interface description methods. These comparisons deal mainly with codes developed in house and implemented using a compiler of choice. Most notably the studies range from the pioneer comparisons of Scardovelli and Zaleski (1999) and Pilliod and Puckett (2004) to more recent studies by: Klostermann *et al*. (2012); Aniszewski *et al.* (2014); Caron *et al.* (2014); Cifani *et al.* (2016).

Aniszewski *et al.* (2014) compare 4 types of advection methods in the CLSVOF (Coupled Level Set Volume of Fluid) framework. The algorithms compared are: the CLSVOF; the THINC/SW method (Tangent of Hyperbola Interface Capturing with Slope Weighting); the WLIC method (Weighted Linear Interface Calculation); and, the PLIC method (Piece-wise Linear Interface Calculation). The basic difference is that CLSVOF and PLIC use geometric interface reconstruction, different from methods THINC/SW and WLIC, which does not require such geometric reconstruction, i. e., does not need to calculate the slope of the interface, using only weighted functions (WLIC) or a tangent fitted curve (THINC/SW). All methods are implemented using FORTRAN, and the comparison was done by measuring mass conservation, spurious currents, parasitic currents, CPU time and number of code lines. Aniszewski *et al.* (2014) point out that all methods have their own advantages and disadvantages. As methods THINC/SW and WLIC are simpler, they require much less computational lines and then their use would be preferable in the first attempts for a programmer to study a two-phase flow. Furthermore, using THINC/SW or WLIC VOF methods coupled with Level Set retrieves much more accurate results concerning the mass conservation then using Level Set alone. When simulating surface tension dominated flows or highly fragmented interface flows, CLSVOF and PLIC can be less expensive than using THINC/SW and WLIC, as the latter requires refined grids. Overall, the differences between THINC/SW and WLIC and between CLSVOF and PLIC are much smaller then between CLSVOF or PLIC and THINC/SW or WLIC.

Caron *et al.* (2014) show a comparison of the dam break problem between experimental data and numerical simulations using the VOF model. The comparison is focused on the turbulence models available, comparing the results with the experimental results. The results show the turbulence models introduce a diffusive effect that helps in the control of the interface evolution. This effect allows obtaining a mesh independent solution with less volumes.

Cifani *et al*. (2016) compare two VOF advection methods using openFOAM, a high order differential scheme (the surface compression method) and the PLIC (implemented as a user-defined function). The rising air bubble inside a viscous fluid test problem was considered, and the authors concluded that, although the compression method always conserves mass and is less computationally expensive, its results are not as accurate. The authors speculate that the main reason is interface numerical diffusion problems. The PLIC shows a 2nd order convergence rate in most of the test cases, high accuracy in describing the interface and a very small mass imbalance. Cifani *et al*. (2016) also point out that the combination of the VOF-PLIC with a surface tension computation using a smoothing technique shows the best results (both in accuracy and grid refinement convergence analysis).

2. MODELING

The tracking of the interface between the phases is accomplished by solving a continuity equation for the volume fraction of each of the phases. For the

q^{th} phase, this equation has the following form:

$$\frac{\partial(\alpha_q \rho_q)}{\partial t} + \nabla \cdot (\alpha_q \rho_q \vec{v}_q) = S_{\alpha_q} + \sum_{p=1}^{n} (\dot{m}_{pq} - \dot{m}_{qp}) \quad (1)$$

In which: α_q is the q^{th} phase volume fraction, $\dot{m}_{pq}$ is the mass transfer from phase p to phase and $\dot{m}_{qp}$ is the mass transfer from phase q to phase p. The source term on the right-hand side of Eq. (1), S_{α_q} is usually zero, but it can be specified to be a mass generation term due to any chemical reaction in the bulk of each phase.

After properly solving the transport equations and volume fraction equations, the algorithm of the VOF model must reconstruct the interface between the phases and propagate such interface. These two steps are so important in the VOF model that usually the VOF method is said to be divided in two steps: reconstruction of the interface, and advection of the interface (Parker and Youngs, 1992; Rider and Kothe; 1998; Scardovelli and Zaleski, 1999; Pilliod and Puckett, 2004). Specific algorithms perform each of these steps, and special attention is given to the reconstruction, because this step dictates the resolution of the interface. For the advection there are two algorithms, the operator split and the unsplit, as explained by Scardovelli and Zaleski (1999) to be respectively, explicit and implicit temporal algorithms.

An interfacial surface can be geometrically represented in several ways (Whitman, 1974). In the VOF method, the interface itself is not tracked, instead, the procedure consists of evolving the material volume through each computational cell in time and reconstructing the interface. The reconstruction is based on solving the motion equations, comprising the conservation equations of mass and momentum for transient, incompressible flow of Newtonian fluids.

The conservation of mass in an interface with no phase change or mass transfer establishes that:

$$\vec{v}_q \cdot \hat{n} = V \quad (2)$$

The motion of the interface is described by the volume fraction equation (Eq. (1) with no source term, no mass transfer and for an incompressible flow) and may be written as,

$$\frac{\partial \alpha_q}{\partial t} + \vec{v}_q \cdot \nabla \alpha_q = 0 \quad (3)$$

The software adopted, ANSYS-FLUENT (*ANSYS-FLUENT Solver Theory Guide*, 2017; *ANSYS-FLUENT User Guide*, 2017), uses a whole domain formulation for solving equations of motion (in other words, it solves only one set of motion equations for the role domain). The form of the equations of motion appears below, respectively mass and momentum conservation equations,

$$\nabla \cdot \vec{v} = 0 \quad (4)$$

$$\frac{\partial \vec{v}}{\partial t} + \vec{v} \cdot \nabla \vec{v} = -\frac{\nabla p}{\rho} + 2\nabla \cdot \left(\mu \overline{\overline{D}} \right) + 2\sigma\kappa\delta_S \hat{n} \quad (5)$$

in which $\overline{\overline{D}}$ is the rate of shear tensor, and the last term of Eq. (5), $2\sigma\kappa\delta_S\hat{n}$, is due to the surface tension force acting on the interface. The most common surface tension model used in literature is the Continuum Surface Force – CSF model proposed by Brackbill *et al.* (1992) and is the procedure adopted in this study. With this model, the addition of surface tension to the VOF calculation results in a source term in the momentum equation (last term in Eq. 5).

The only properties that are not continuous through the interface are density and viscosity. These are calculated respectively by the following expressions,

$$\rho = \sum_{q=1}^{n} (\rho_q \alpha_q) \quad (6)$$

$$\mu = \sum_{q=1}^{n} (\mu_q \alpha_q) \quad (7)$$

As previously said, the application of the VOF method is divided in two steps: interface propagation (advection) and interface reconstruction. The first step of the VOF method is the advection of the interface (or the volume fractions), it is meant to determine how the interface will evolve between two consecutive time steps. The second step is to reconstruct the interface, and it is meant to determine the shape, orientation and current position of the interface at the end of any given time step. This is performed using the solution of the motion equations (mass and momentum conservation equations) along with the volume fraction advection equation (Eq. 3).

The advection of the interface is determined by solving the motion equations based on the shape, orientation and the position of the interface at the beginning of any given time step. This process must avoid the interface smearing, so the numerical solution must guarantee low levels of numerical diffusion. According to the *ANSYS-FLUENT Solver Theory Guide* (2017), three basic methods for advection can be found in literature: the original donor-acceptor scheme (algorithm splitting) presented by Hirt and Nichols (1981), which computes the face fluxes in each direction separately; the high-order differencing schemes such as the CICSAM (Compressive Interface Capturing Scheme for Arbitrary Meshes) presented by Ubbink (1997), or the unsplit algorithm that computes the face fluxes in all directions at once; and the line techniques, which are, in essence, improvements in the donor-acceptor scheme. The line techniques differ from the donor-acceptor scheme in the fact that the fluxes for each phase are weighted depending on the inclination of the line (or plane in 3D) that separates the phases inside each cell (*ANSYS-FLUENT Solver Theory Guide*, 2017). Each of these employs its own

reconstruction technique.

The ANSYS-FLUENT software offers two integration procedures for Eq. (3), implicit (available for transient and steady state simulations) and explicit (for transient simulations only). The great advantage of the implicit integration is that, when only the steady state solution is desired, the use of the implicit integration process can be much more computationally efficient and less time demanding, while the explicit integration demands for the solution of the full transient flow. The implicit integration can also be used for establishing initial conditions for transient simulations, speeding up the process.

The methodologies to be compared in this study are the following: Geometric Reconstruction (based on the PLIC – Piecewise Linear Interface Construction), which is a line technique; the CICSAM, the HRIC – High Resolution Interface Capturing, the Compressive Scheme, the Bounded Gradient Maximization Scheme – BGM, are high-order differencing schemes; and the UPWIND Interpolation Scheme based on the donor-acceptor scheme. The use of the Geometric Reconstruction and the CICSAM algorithms are limited to transient simulations because these are based on the explicit solution for the interface (operator splitting method). The HRIC and the UPWIND schemes can be used within both transient and steady state simulations, using the splitting operator for the transient calculations and an implicit unsplit operator scheme for steady state. The BGM scheme can only be used for steady state simulations. These methodologies are extensively described in several texts in literature (Parker and Youngs, 1992; Ubbink, 1997; Rider and Kothe; 1998; Scardovelli and Zaleski, 1999; Muzaferiju and Peric, 2000; Pilliod and Puckett, 2004; Walters and Wolgemuth, 2009) and will not be extensively discussed here.

3. SOLUTION VALIDATION

To validate the numerical solutions obtained using ANSYS-FLUENT, the single rising bubble in a viscous liquid was chosen as benchmark. The Geometric Reconstruction algorithm was used for both simulated cases, because this method will be used for creating the reference solution of the dam break problem. The study by Klostermann *et al.* (2013) is used for comparisons. This study was compared with other numerical simulations (for interface form and bubble rise velocity) and with experimental data (for bubble rise velocity). The numerical parameters for the simulations were the same as in the original study, with a regular grid spacing of 3.125 mm and 1.5625 ms as time interval. The conditions, physical properties and dimensionless numbers for the simulations are shown in Table 1.

Figure 1 shows the comparison of interface form for case TC1. The comparison shows the two solutions are almost coincident. The results of Klostermann *et al.* (2013) are shown in triangles and the current approach is displayed as small dots. Although the grid used is the same (3.125 mm regular spacing), the results of Klostermann *et al.* (2013) are shown as few points due to the lack of the original data for comparison. These points were captured with an in house code that allows for the capturing of discrete points in digital images.

Table 1 Physical properties and dimensionless parameters for the rising bubble simulations

	Case TC1	Case TC2
ρ_1	1000	1000
ρ_2	100	1
μ_1	10	10
μ_2	1	0.1
g	0.98	0.98
σ	24.5	1.96
Re	35	35
Eo	10	125
Ca	0.286	3.571

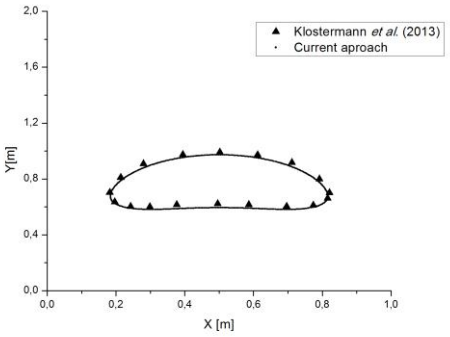

(a)

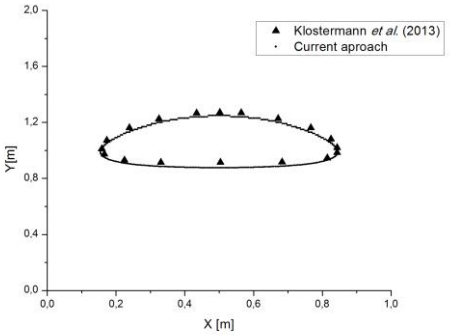

(b)

Fig. 1. Comparison with the study by Klostermann *et al.* (2013) at 1.5 s (a) and 3.0 s (b) for the TC1 case.

Figure 2 shows a comparison analogous to that of Fig. 1, with the conditions, physical properties and dimensionless numbers for case TC2. The figure shows the current results as small dots and the reference simulation (Klostermann *et al.*, 2013) as triangles. The simulation using the

ANSYS-FLUENT (current approach) was able to reproduce the results of Klostermann *et al.* (2013), including the bubble break-up at the edges and the trailing small bubbles in each tip of the main bubble.

With this results, the solutions for the dam break problem can now be addressed with confidence, and the ANSYS-FLUENT software will be able to deal with the interfacial break-up and reconnection, while still being able to correctly represent the interface evolution.

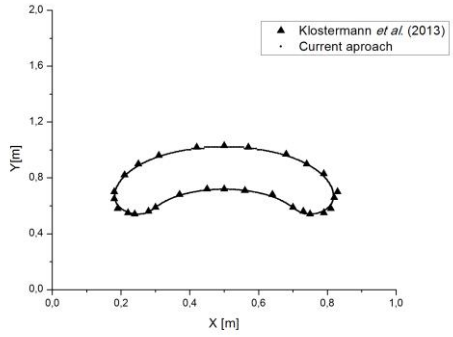

(a)

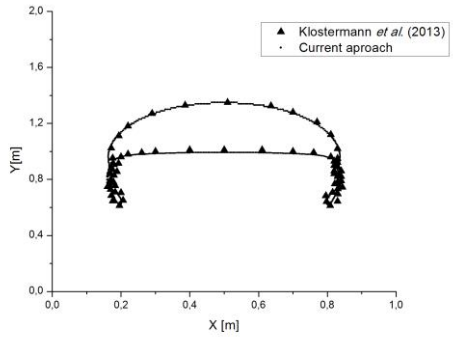

(b)

Fig. 2. Comparison with the study by Klostermann *et al.* (2013) at 1.5 s (a) and 3.0 s (b) for the TC2 case.

4. RESULTS AND DISCUSSION

The dam break problem is simulated using a two-dimensional domain of 1000 mm in length and 200 mm high. Four different uniform quadrilateral grids were used for this analysis. Table 2 specifies each of the computational grids with a reference number for future use. The time step is chosen to be equal to 1 ms, and the simulations are performed for 10 thousand time steps (near the steady state) while allowing for 100 interactions to be performed within each time interval. The boundary and initial conditions are shown in Fig. 3. The solution methods and under-relaxation parameters were kept at the default settings.

Table 2 Naming of computational grids used for simulation and comparison

Grid Number	Grid Division	Thousands of Computational Cells
1	100 x 20	2
2	200 x 40	8
3	400 x 80	32
4	800 x 160	128

A single geometric reconstruction (PLIC) simulation with 512 thousand volumes (1600 x 320 computational cells) was executed and is taken as the benchmark for comparison with all other simulations. In this benchmark simulation, the time step was also reduced to 0.1 ms, while also allowing for 100 interactions within each time step. The default settings for solution methods and under-relaxation parameters were maintained. Figure 4 shows a grid refinement assessment for all the simulated grids using the geometric reconstruction (PLIC) and demonstrates that the simulation with grid 4 and the reference grid of 512 thousand volumes present the same results. Figure 5 shows the reference simulation in several time steps (from 0.5 s to 1.9 s).

After starting the simulation, water runs through the base wall and reaches the right wall (sloshing) near the 0.5 s mark. At the 0.7 s, the water front falls back to the bottom wall. After the impact between the water front and the liquid film at the bottom wall, the mixing phenomenon is apparent. The air bubbles became entrapped into water, revealing a highly nonlinear interaction between the phase advection and the velocity field. This entrance of air inside the water phase continues until the phase separation starts to become prominent near the steady state. As one of the focuses of this study is to investigate the quality of the interfacial representation, the result analysis will be concentrated between the instants 1.0 s and 1.3 s.

For the steady state simulations, all default parameters were maintained; however, the steady state calculations performed by ANSYS-FLUENT software are in fact pseudo-transient simulations, with a distorted time advancement. The procedure is to advance time while not fully converging each time interval. A time scale is provided to the software along with a Courant number and a maximum simulated time (*ANSYS-FLUENT Solver Theory Guide*, 2017; *ANSYS-FLUENT User Guide*, 2017). Thus, the software advances time rapidly, providing a stable and fast steady state answer. This procedure is useful when complex simulations are necessary and when the initial transient is not required. Advancing the simulation rapidly can save precious computational time and allow for more simulation results to be produced.

Figures 6 and 7 show qualitative comparisons of the interface resolution. The figures show the explicit schemes had better qualitative interface resolution than the implicit schemes. The PLIC and CICSAM schemes show almost the same results, and the

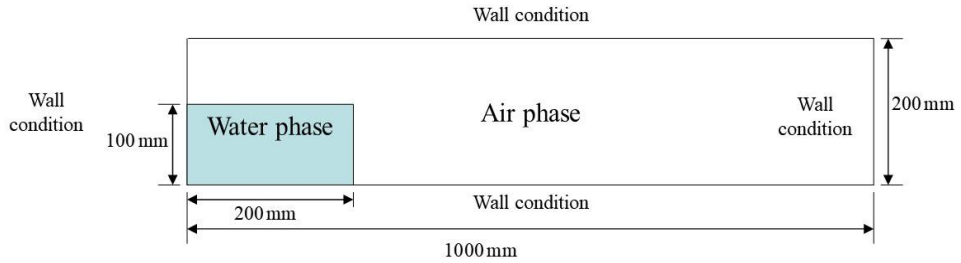

Fig. 3. Boundary and initial conditions for the dam break problem.

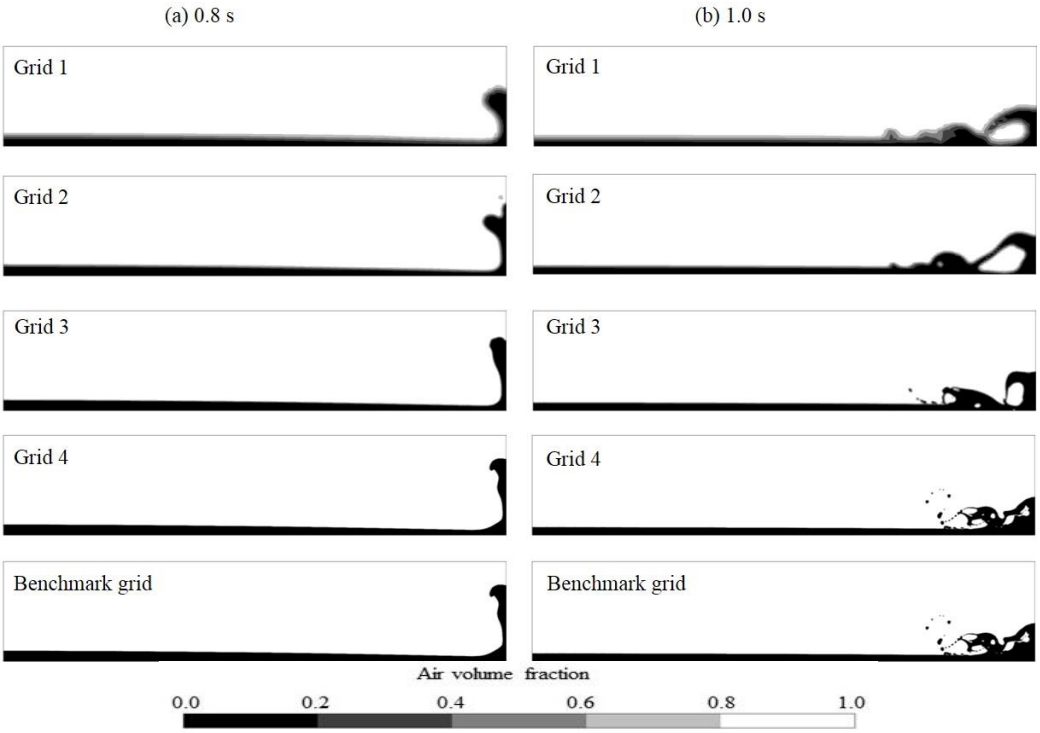

Fig. 4. Assessment of grid refinement for two distinct times (a) at 0.8s; (b) 1.0 s.

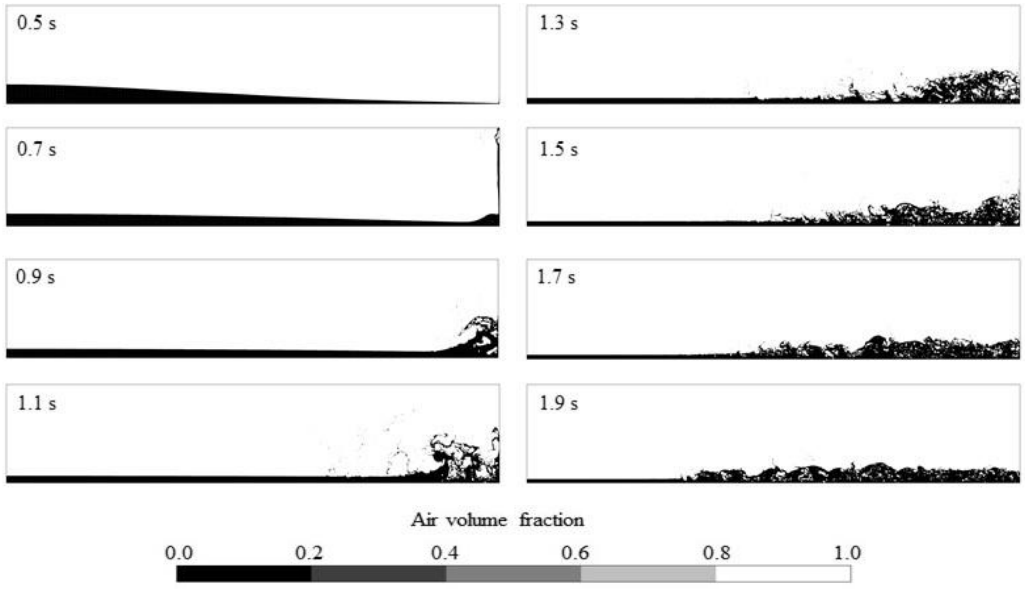

Fig. 5. Time evolution for the dam-break problem using the geometric reconstruction scheme (PLIC) for a reference mesh of 512 thousand computational cells.

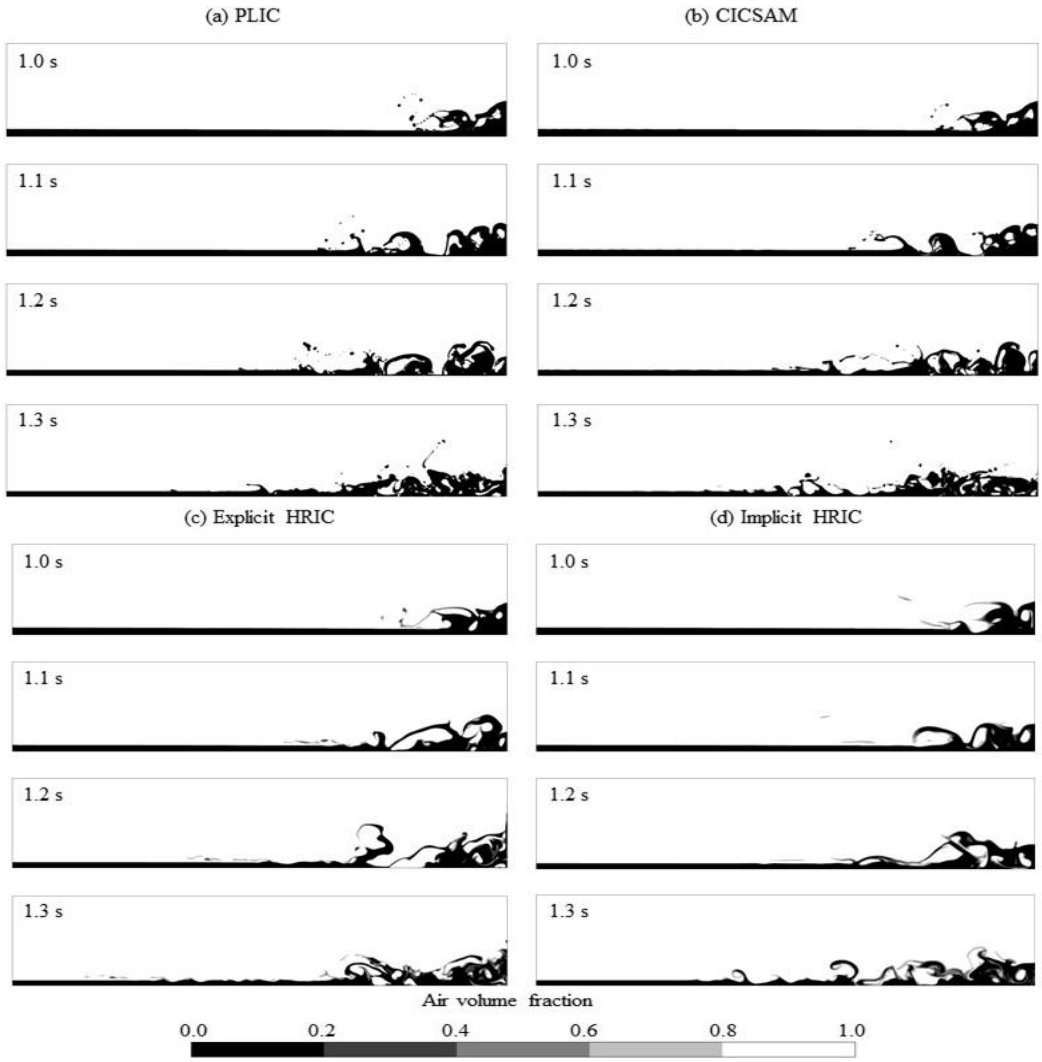

Fig. 6. Comparison between (a) PLIC, (b) CICSAM, and HRIC both (c) explicit and (d) implicit schemes using grid 4.

results of HRIC explicit scheme are better than those of the implicit one. The UPWIND scheme presents major diffusion issues. The interface smearing is the most notable in the thin liquid filaments that splash from the impact of the falling liquid front and the film on the bottom wall. This can be seen in the continuous gray areas that demonstrate the existence of regions with intermediate water fractions. This evidences a mass imbalance that will be demonstrated later.

To demonstrate that this phenomenon depends on the grid (thus attributed to numerical diffusion), Fig. 8 shows the comparison of all transient simulations (for grids 1 to 4) using the 1.2 s time frame as a base. The results of the PLIC and the CICSAM are almost the same for the representation of the interface in grids 3 and 4, while for grids 1 and 2 the resolution of PLIC is slightly better than that of CICSAM. These results demonstrated that even for grid 4 the implicit schemes present poor resolution with a smeared interface (highly diffused/smeared interface), mainly for the UPWIND interpolation. A mass conservation verification is then performed to evidence quantitatively the numerical diffusion.

Figure 9 shows a mass imbalance calculation. In these results the total mass of water between the initial and final time steps is compared. The comparison is made using a dimensionless mass loss variable, Δm^*, defined as:

$$\Delta m^* = \left(\frac{m_f - m_i}{m_i} \right) 100 \tag{8}$$

In which m_f is the total amount of water for the final time step and m_i the total initial amount of water.

The mass loss reached a maximum value of 0.072 % for the UPWIND scheme with grid 1. The explicit HRIC scheme conserved mass for both grids 1 and 2 and, although not visible, it gained a little amount of mass for grids 3 and 4 (equal to 5×10^{-5} % and 10^{-4} %, respectively). CICSAM also had no mass loss or gain for grid 1 and presented a peak in mass loss for grid 2. For grids 3 and 4, the CICSAM presented little mass imbalance, in the

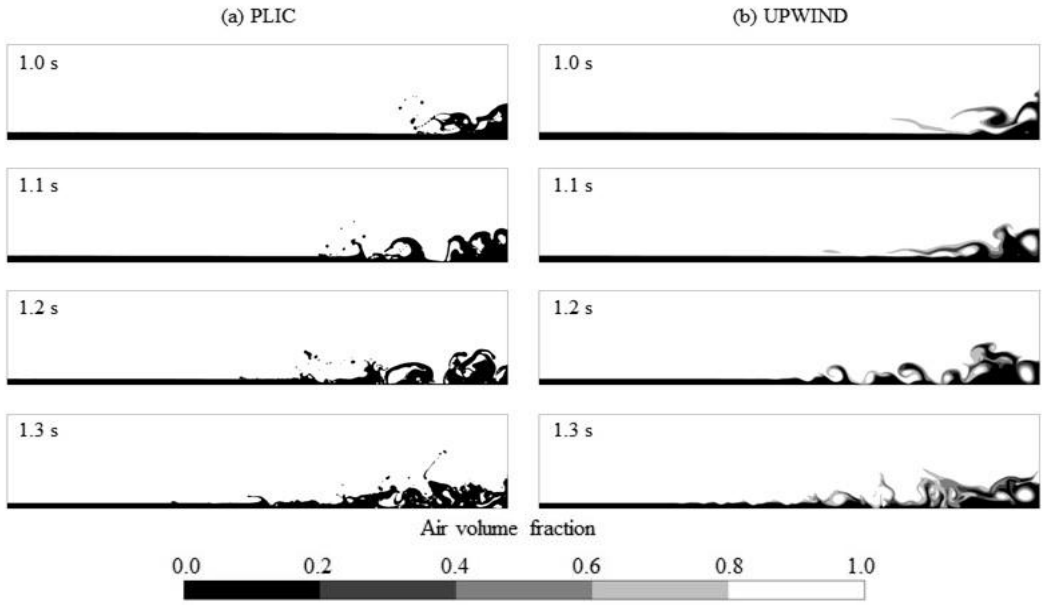

Fig. 7. Comparison between PLIC and UPWIND schemes using grid 4.

order of 10^{-4} %. The PLIC algorithm conserved mass in all grids.

Overall, although the non conservation of mass is very discrete, it demonstrates that the implicit schemes, especially the UPWIND scheme, are not reliable for both qualitative (as previous analyzed) and quantitative aspects during transient simulations. The simulations with the implicit schemes showed greater mass loss for grid 4 than grid 3, probably due to an increased Courant number when using a smaller mesh division. To allow seeing whether the mass loss would be diminished by using smaller time steps, more simulations and further studies would be necessary.

To explore the capabilities of the ANSYS-FLUENT software, distorted transient simulations (steady state simulations) were also performed. These simulations aim to demonstrate that if only steady state results are required, an implicit scheme with a compressive interpolation function may be a viable option. Other uses for this type of algorithm is in the development of initial conditions for complex simulations in which only the final transient behavior (or the perturbation of any given state) is required. For grids 1 and 2 the pseudo time step set was 1 ms, and the simulations were stable. For grid 3, this parameter had to be reduced to 0.1 ms, while for grid 4 a 10 μs pseudo time step had to be used for a stable simulation.

Figure 10 shows the comparison of the three steady state interpolation methods available in the ANSYS-FLUENT software. The reference final (steady state) result is the last frame of Fig. 2. The BGM scheme produces a very sharp interface resolution for all grids except for grid 1, which shows a little interface smearing. The compressive scheme also produces a sharp interface for grids 3 and 4, while presenting visible interface smearing in grid 1 and a slight diffusion for grid 2. The modified HRIC scheme is not able to generate a sharp interface for any of the grids investigated. For both the BGM and the compressive schemes, the pseudo time step interval had to be reduced for a stable simulation. The sharpness of this result is impressive and encourages the use of the pseudo-transient algorithm to obtain a steady state solution or to generate initial conditions when useful.

The computation time for all transient simulations are within the same order of magnitude. A 5% spreading of elapsed simulation times may be attributed to the processing cores used for the simulations being requested by other processes. Isolating and quantifying this influence is difficult, as the simulations were run in a Windows workstation that runs several processes in the background. The mean elapsed time for the transient results using each grid is shown in the first line of Table 3 normalized by the time spent for the simulation of the most demanding grid. The other 3 lines present the elapsed time for each of the grids when the pseudo-transient (steady state) simulations were run. The results are normalized to the mean elapsed time from the transient simulation for grid 4. From this perspective, if only steady state results are pursued (or obtaining initial conditions), the use of the distorted transient is important. The BGM method approaches the computation time for the transient simulation (around 60% of the total time) due to a severe increase in the Courant number. Other factors contributing to this phenomenon could not be identified.

Figure 8 shows the mass imbalance calculation for the pseudo-transient simulations. A poor result is achieved for the coarser grids (grids 1 and 2). For grid 3 the BGM and the compressive interpolation schemes fall below the 1.0 % mark, while the modified HRIC stays just above it with approximately 1.06%. For grid 4 the compressive scheme becomes unstable (probably because of the high numerical diffusion due to an elevated local

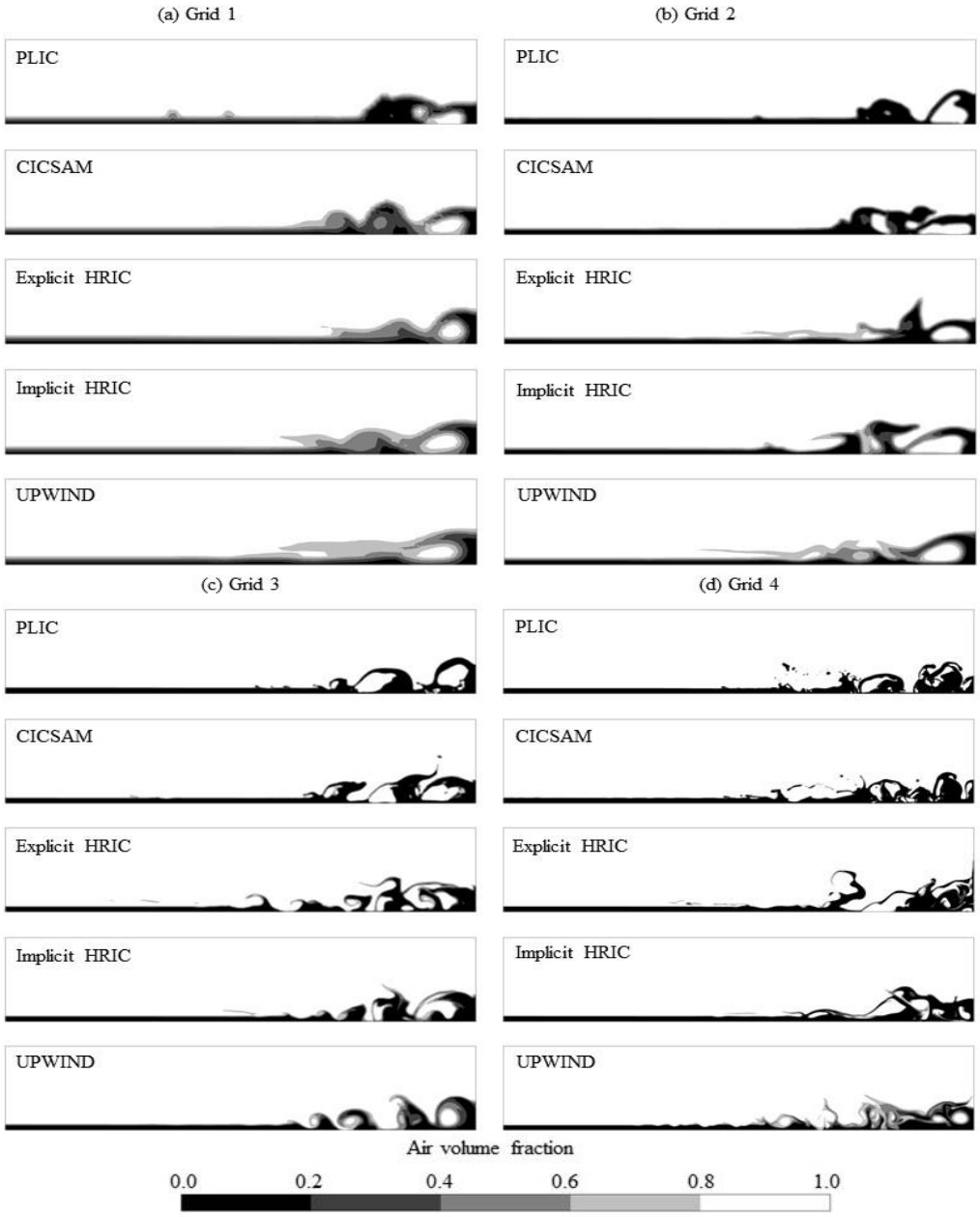

Fig. 8. Comparison between all schemes for 1.2 s. Grids 1, 2, 3, and 4.

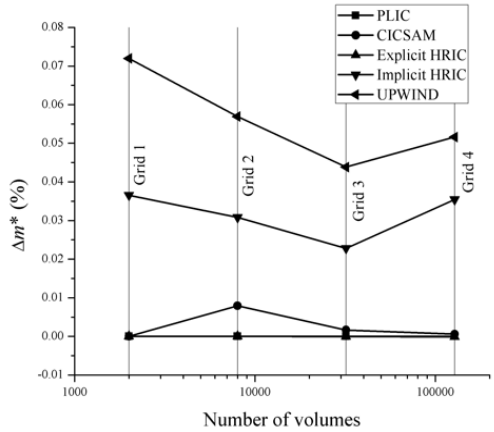

Fig. 9. Mass imbalance for each grid and interpolation scheme for transient simulations.

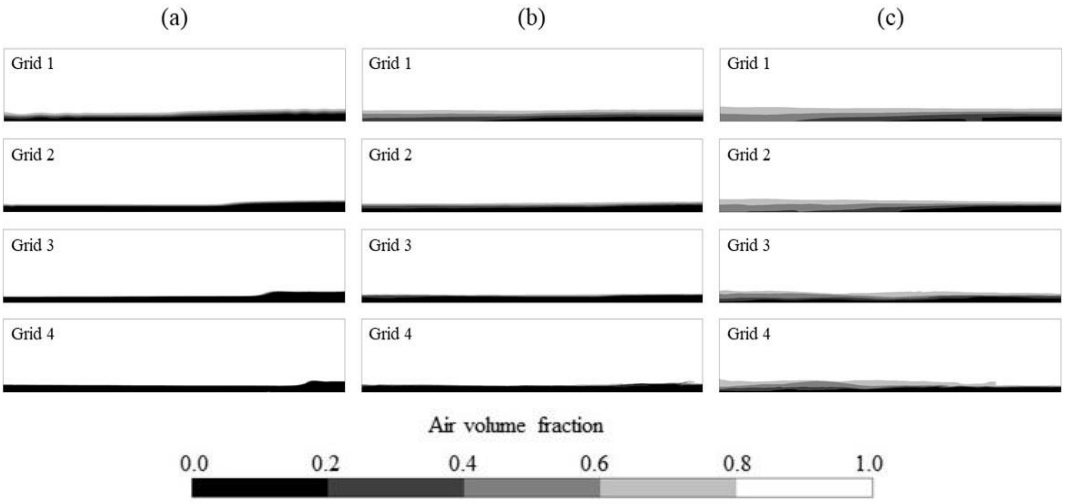

Fig. 10. Comparison between (a) BGM, (b) compressive and (c) modified HRIC schemes.

courant number) and the mass imbalance rises to about 5%. The mass imbalance for the other interpolation schemes approaches zero for grid 4.

Table 3 Normalized elapsed time of each grid for the transient mean and steady state simulations

	Grid 1	Grid 2	Grid 3	Grid 4
Transient – mean	0.084	0.215	0.742	1.000
BGM	0.007	0.009	0.014	0.595
Compressive	0.002	0.003	0.004	0.007
HRIC	0.002	0.003	0.004	0.009

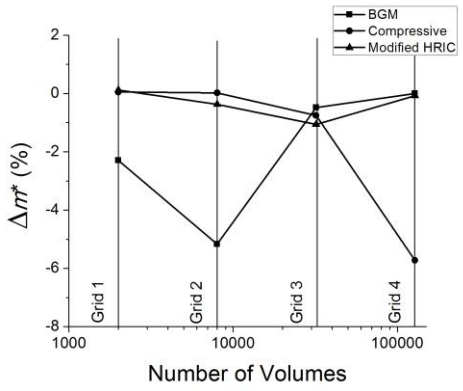

Fig. 11. Verification of the mass conservation for the steady state simulations.

5. CONCLUSION

The main conclusion of this study is that the modified HRIC and the performance of CICSAM interpolation schemes is analogous to the Geometric Reconstruction (PLIC) in grids 3 and 4. The main advantages of the PLIC appear in the coarser meshes (2,000 and 8,000 volumes) that showed great advantage for the explicit PLIC solution. The PLIC algorithm was much more capable of representing the interface even for a coarse mesh. This makes the PLIC the most feasible method of interpolating the interface available in the ANSYS-FLUENT for transient simulations. The stability of the interpolation schemes is highly connected to the maximum local Courant number in all cases, including the implicit and the pseudo-transient simulations.

As the simulation times are in the same order of magnitude, there is no incentive to use an interpolation scheme other than the Geometric Reconstruction (PLIC) for transient simulations. For the pseudo-transient simulations, aiming for the steady state solution for the problem (or to obtain an initial condition with little computation time) the use of the implicit schemes is advised. The compressive scheme has a slightly better computation time, but for other types of problems this might be opposite.

The way forward for this study is the assessment of interfacial anti-diffusion mechanisms that are present in the commercial software investigated. They may impact the way the implicit algorithms respond to the mesh refinement. Another important aspect of the solution that can be explored is the coupled level-set – VOF algorithm, which computes the gradients and derivatives in the numerical solution using a level-set function and calculates the position of the interface using the VOF model.

As a final recommendation, when studding an unknown problem, performing a fully transient simulation as a start is advised. Once the characteristics of the problem have been explored, the decision of using the pseudo-transient approach can be explored further. Great applications of this type of approach using the pseudo-transient simulation for optimization processes and for developing several initial conditions for transient analysis of a set of conditions.

ACKNOWLEDGEMENTS

The authors would like to thank Prof. Paulo Sergio Berving Zdanski for allowing the use of the computational facilities in the Thermal Sciences Laboratory at the College of Technological Sciences of the Santa Catarina State University at Joinville. Great thanks also to FAPESC for the financial support provided to the University in general.

REFERENCES

Alves, M. V. C., J. R. Barbosa and A. T. Prata (2013). Analytical and CFD modeling of the fluid flow in an eccentric-tube centrifugal oil pump for hermetic compressors. *International Journal of Refrigeration-Revue Internationale du Froid* 36 (7) 1905-1915.

Alves, M. V. C., J. R. Barbosa and A. T. Prata and F. A. Ribas Jr., (2011). Fluid flow in a screw pump oil supply system for reciprocating compressors *International Journal of Refrigeration* 34 (2011), pp. 74-83

Aniszewski, W., T. Menard and M. Marek (2014). Volume of Fluid (VOF) type advection methods in two-phase flow: A comparative study. *Computers & Fluids* 97 52–73.

ANSYS-FLUENT Solver Theory Guide. (2017).

ANSYS-FLUENT User Guide. (2017).

Batchelor, G. K. (1967). *An introduction to fluid dynamics*. Cambridge USA, University Press.

Bilger, C., M. Aboukhedr, K. Vogiatzaki, and R. S. Cant (2014). Evaluation of two-phase flow solvers using Level Set and Volume of Fluid methods. *Journal of Computational Physics* 345 (2017) 665–686.

Bortolin, S., E. Da Riva and D. Del Col (2014). Condensation in a square minichannel: application of the VOF method. *Heat Transfer Engineering* 35 (2), 193–203.

Brackbill, J. U., D. B. Kothe, and C. Zemach (1992). A continuum method for modeling surface tension. *Journal of Computational. Physics*100, 335-354.

Caron, P. A, M. A. Cruchaga, A. E. Larreteguy (2015). Sensitivity analysis of finite volume simulations of a breaking dam problem. *International Journal of Numerical Methods for Heat & Fluid Flow* 25(7), 1718-1745.

Cifani, P. , W. R. Michalek, G. J. M. Priems, J. G. M. Kuerten, C. W. M. van der Geld and B. J. Geurts (2016). A comparison between the surface compression method and an interface reconstruction method for the VOF approach. *Computers & Fluids* 136, 421-435.

Da Riva, E. And D. Del Col (2009). Numerical simulation of churn flow in a vertical pipe. *Chemical Engineering Science* 64, 3753–3765.

Gaskell, P. H. and A. K. C. Lau (1998). Curvature-compensated convective transport: SMART, a new boundedness-preserving transport algorithm, *International Journal for Numerical Methods in Fluids* 8, 617–641.

Hernandez-Perez, V., M. Abdulkadir, B. J. Azzopardi (2011). Grid generation issues in the CFD modelling of two-phase flow in a pipe. *The Journal of Computational Multiphase Flows* 3, 13–26,

Hirt, C. W. and B. D. Nichols (1981). Volume of fluid (VOF) method for the dynamics of free boundaries. *Journal of Computational Physics* 39 (1): 201–225.

Hirt, C. W. and B. D. Nichols (1988) Flow-3D users' manual. *Technical Report, Flow Sciences, Inc.*

Horgue, P., F. Augier, M. Quintard and M. Prat (2012). A suitable parametrization to simulate slug flows with the Volume-of-Fluid method. *Comptes Rendus Meca* 340:411–419.

Karami, H., C. F. Torres, M. Parsi, E. Pereyra and C. Sarica (2014). CFD Simulations of Low Liquid Loading Multiphase Flow in Horizontal Pipelines., ASME 2014 4th Joint US-European Fluids Engineering Division Summer Meeting collocated with the ASME 2014 12th International Conference on Nanochannels, Microchannels, and Minichannels, At Chicago, Illinois, USA, Volume: 2

Kashid, M. N., A. Renken and L. Kiwi-Minsker (2010). CFD modelling of liquid–liquid multiphase microstructured reactor: slug flow generation. *Chemical Engineering Research and Design* 88, 362–368.

Klostermann, J., K. Schaake and R. Schwarze (2013). Numerical simulation of a single rising bubble by VOF with surface compression. *International Journal for Numerical Methods in Fluids* 71:960–982.

Magnini, M., B. Pulvirenti and J. R. Thome (2013). Numerical investigation of hydrodynamics and heat transfer of elongated bubbles during flow boiling in a microchannel. *International Journal of Heat and Mass Transfer* 59, 451–471.

Minussi, R. B. and G. D. Maciel (2012). Numerical Experimental Comparison of Dam Break Flows with non-Newtonian Fluids. *Journal of the Brazilian Society of Mechanical Sciences and Engineering* 34 (2), 167-178

Muzaferiju, S. and M. Peric (2000). A two-fluid Navier-Stokes solver to simulate water entry. in: *22nd Symposium on Naval Hydrodynamics*, pages 638.651.

Leonard, B. P. (1991). The ULTIMATE conservative difference scheme applied to unsteady one-dimensional advection, *Computer Methods in Applied Mechanics and Engineering* 88, 17–74.

Lückmann, J. A., M. V. C. Alves and J. R. Barbosa Jr., (2009). Analysis of oil pumping in a reciprocating compressor *Applied Thermal Engineering* 29 (2009), 3118-3123

Parker, B. J., and D. L. Youngs (1992) *Two and three-dimensional Eulerian simulation and fluid flow with material interfaces.* Technical Report, UK Atomic Weapons Establishment.

Pilliod, J. E. and E. G. Puckett (2004). Second order accurate volume-of-fluid algorithms for tracking material interfaces. *Journal of Computational Physics* 199, 465–502.

Rezende, R. V. P., R. A. Almeida, A. A. U. Souza, U. Guelli and S. M. A. Souza (2014). A two-fluid model with A tensor closure model approach for free surface flow simulations. *Chemical Engineering Science* 122, 596-613.

Ratkovich, N., S. K. Majumder, T. R. Bentzen (2013). Empirical correlations and CFD simulations of vertical two-phase gas–liquid (Newtonian and non-Newtonian) slug flow compared against experimental data of void fraction. *Chemical Engineering Research and Design* 91, 988–998.

Rider, W. J. and D. B. Kothe (1998) Reconstructing volume tracking. *Journal of Computational Physics* 141, 112-152.

Saad, S. B., C. Gentric, J. F. Fourmigué, P. Clément and J. P. Leclerc (2014). CFD and experimental investigation of the gas–liquid flow in the distributor of a compact heat exchanger. *Chemical Engineering Research and Design* 92 (11), 2361–2370.

Scardovelli, R. and S. Zaleski (1999) Direct numerical simulation of free-surface and interfacial flow. *Annual Reviews of Fluid Mechanics* 31, 567-603.

Soleymani, A., A. Laari and I. Turunen (2008). Simulation of drop formation in a single hole in solvent extraction using the volume-of-fluid method. *Chemical Engineering Research and Design* 86, 731–738.

Ubbink, O. (1997). *Numerical Prediction of Two Fluid Systems with Sharp Interfaces*. PhD thesis. Imperial College of Science, Technology and Medicine, London, England.

Walters, D. K. and Wolgemuth, N. M. (2009). A new interface-capturing discretization for numerical solution of the volume fraction equation in two-phase flows. *International Journal for Numerical Methods in Fluids* 60. 893-918.

Whitham G. 1974. Linear and Non-Linear Waves. New York: Wiley-Interscience.